J Mater Sci (2010) 45:624–632
DOI 10.1007/s10853-009-3936-3

Degradation behaviour and mechanical properties of magnesium implants in rabbit tibiae

Annett Krause · Nina von der Höh · Dirk Bormann · Christian Krause · Friedrich-Willhelm Bach · Henning Windhagen · Andrea Meyer-Lindenberg

Received: 4 June 2009 / Accepted: 29 September 2009 / Published online: 14 October 2009

Abstract To investigate the initial mechanical strength and the degradation behaviour with the associated changes in mechanical properties of magnesium-based osteosynthesis implants, 30 rabbits were implanted with cylindrical pins of the alloys MgCa0.8 (magnesium with 0.8 wt% calcium), LAE442 (magnesium with 4 wt% lithium, 4 wt% aluminium and 2 wt% rare earths) and WE43 (magnesium with 4 wt% yttrium and 3 wt% rare earths). The implants were inserted into the medullary cavity of both tibiae. After 3 and 6 months, each half of the animals was euthanized, respectively, and the implants were taken out. A determination of volume, three-point bending tests, scanning electron microscopy (SEM) and energy dispersive X-ray analyses as well as metallographic and μ-computed tomography examinations were accomplished. All implants were clinically well tolerated. MgCa-implants showed the least initial strength and the highest loss in volume after 6 months. SEM- and μ-computed tomography examinations revealed a pronounced pitting corrosion. Therefore, their use as degradable implant material seems to be limited. LAE442 has the best initial strength which seems to be sufficient for an application in weight-bearing bones. The degradation behaviour is very constant. However, possible unknown side effects of the rare earths have to be excluded in further investigations on biocompatibility. Considering all results of WE43, its application as osteosynthesis material for fracture repair is ineligible due to its heterogeneous and unpredictable degradation behaviour.

A. Krause · N. von der Höh (✉) · A. Meyer-Lindenberg
Small Animal Clinic, University of Veterinary Medicine Hannover, Bischofsholer Damm 15, 30173 Hannover, Germany
e-mail: nina.von.der.hoeh@tiho-hannover.de

D. Bormann · C. Krause · F.-W. Bach
Institute of Materials Science, University of Hannover, An der Universität 2, 30823 Garbsen, Germany

H. Windhagen
Department of Orthopaedics, Medical University of Hannover, Anna-von-Borries-Straße 3, 30625 Hannover, Germany

Introduction

In human medicine just as in animal health, mainly titanium and steel as non-resorbable, metallic-osteosynthetic materials are used for the treatment of fractures [1–5]. These materials show much higher stiffness than bone [6–8]. As a result, a stress shielding emerges which prevents the healing of the fracture, the physiological stimulation of the bone tissue and thus, the re-shaping of the bone [1, 9]. Furthermore, these materials have to be removed very often in a second surgery due to implant loosening and foreign body and/or allergic reactions. An alternative to the above-mentioned materials could be resorbable, metallic implants based on magnesium. Magnesium and its alloys have a similar Young's modulus and a favourable compression and tensile strength in relation to the cortical bone [10, 11]. Regarding fracture treatment, magnesium alloys would have the advantage that the implant provides an adapted stabilization of the curing bone depending on its own state of stability. Such a strain adaption can optimize the bone transformation according to Wolff's law [12–14]. Furthermore, no second surgery would be necessary due to the ideally total resorption of the implant. So the strain for the patient as well as the treatment expenses could be reduced significantly.

Up to now, the medical use of magnesium has been limited owing to the fast degradation and the undesirable generation of gas. At the beginning of the twentieth

century, Verbrugge [15] used a magnesium alloy with 8 wt% aluminium as osteosynthetic material in human medicine: The implant dissolved completely during the healing process. He also observed a significant emergence of gas. Contemporary investigations with the magnesium alloys AZ31, AZ91, WE43 and LAE442 in the femur of Guinea pigs also showed an emergence of gas with the least gas generation in LAE442 followed by WE43 [16]. Investigations on extruded implants of LAE442 and WE43 in the tibiae of rabbits showed different results. For both alloys, no generation of gas could be proved clinically and radiographically [17]. By alloying other components like calcium or rare earth elements, new potentials in the in vivo use of magnesium alloys arose [18].

For osteosynthesis in weight-bearing bones, surgical implants require a sufficient strength. Especially degrading materials whose strength decreases with increasing degradation an adequate initial strength and an adapted loss in strength is very important. For determination of strength, three-point bending tests can be carried out [19, 20]. Resulting values are the maximal applied force (F_{max}) at fracture and the bending displacement at fracture. F_{max} at fracture gives information about the implants' strength, whereas the bending displacement at fracture represents the ductility. Little is known about the mechanical properties of magnesium alloy implant. Meyer-Lindenberg et al. [21] showed that alloying of different elements could actually influence the bending stiffness.

The aim of this investigations was to examine if different resorbable magnesium implant materials provide the required mechanical strength and how their degradation process proceeds. To determine these properties, a determination of volume, three-point bending tests, scanning electron microscopy (SEM) and energy dispersive X-ray analysis (EDX) as well as metallographic and X-ray tomographical analyses were accomplished.

Materials and methods

Implant production and surgery

Three different magnesium alloys were used as implant material: MgCa0.8, a magnesium alloy with 0.8 wt% calcium, and LAE442 (4 wt% lithium, 4 wt% aluminium, 2 wt% rare earths) and WE43 (4 wt% yttrium, 3 wt% rare earths) as magnesium alloys with rare earth elements.

The production process started with casting. The following extrusion of the materials improved their properties [22]. Extrusion allows the generation of a fine-grained, homogeneous microstructure which leads to improved mechanical properties. Besides an increase in strength, it enhances the corrosion resistance of the material by more evenly distributed precipitations [18].

Extrusion was carried out at the laboratory extruding machine David M 168 (Comp. Bühler Matra). This hydraulic-driven vertical extruder works with a maximal press capacity of 0.8 MN. The casting bolts were turned by cutting to a diameter of 28 mm and a length of 50 mm. The samples were homogenized immediately before the extrusion to cause uniformly distributed precipitations and thus, to relieve internal stresses. Furthermore, homogenization leads to an adjustment of grain segregation and dissolution of eutectic structure at the grain boundaries. Since the press capacity results from friction between the sample and the inner surface of the vacuum chamber, molybdenum disulphide as lubricant was used. All previously polished functional surfaces like the matrix and the die were lubricated as well. The resulted extrusion bolt of each magnesium alloy was turned to cylindrical pins of 2.5 mm in diameter and 25 mm in length. Sterilization was carried out using gamma irradiation (Comp. RüschCare, Germany) [18].

The animal experiment was licensed according to the law of animal welfare (509.6-4250/3-04/750).

Thirty adult, female New Zealand White rabbits (mean weight: 3.3 ± 0.17 kg) were chosen as test animals, 10 for each material. The implantation period was 3 and 6 months, respectively, for each half of the animals.

One pin was implanted intramedullary into the cavity of both tibiae of each rabbit and positioned in the middle third of the tibia diaphysis. The pins were inserted through a drill hole (Φ 2.5 mm) using a small plastic rod. The implant location was checked immediately post-operatively by radiographical examinations. During the implantation periods, the animals were checked clinically daily and radiographs of the hind legs were taken weekly in two planes. After 3 or 6 months, the animals were euthanized and the shank bones were explanted. The right tibiae were kept for histological examinations. The left bones were sawed longitudinally and the pins were carefully extracted for subsequent investigations.

Determination of volume

To determine the decrease in volume during the implantation period, the adhering organic material was carefully removed without damaging the metal substrate. For this purpose, the pins were put into a dipping bath of 40% hydrofluoric acid for 5 min. Following this, they were cleaned in distilled water and ethyl alcohol for 10 s each. After air-drying of the pins, water displacement method was used to determine the decrease in volume. A 0.01-mL scaled volumeter was used. Heptane served as fluid due to

its quasi-inert behaviour in regard to magnesium and its low vapour pressure. Each measurement was repeated thrice to detect and avoid incidental errors.

Bathing in hydrofluoric acid created a very thin magnesium fluoride layer on the implants' surface not exceeding a couple of hundred nanometres thickness after 5 min dipping duration. It is presumed that this layer will not influence the results significantly. For each material and implantation period, three pins were examined as well as one pin of each alloy in its initial state.

Three-point bending test

The mechanical strength of the implants was determined using the universal testing machine Z250 (Comp. Zwick, Ulm, Germany). A 10-kN load cell (Comp. Zwick, Ulm, Germany) was used for the measurement of the maximal applied force. All explanted implants of the left tibiae and three pins of each alloy in their initial state were tested. The implants were centrally positioned on two supports of the testing rig (distance between supports is 15 mm).

To eliminate the influence of the stiffness of the machine, a displacement transducer was used. It also determined the bending displacement during the test. The crosshead moved downwards with a constant velocity of 1 mm/min. A sudden drop of force of 10% was defined as fracture criterion. The test was terminated if the fracture criterion was fulfilled or if the bending displacement reached a distance of 5 mm.

The maximal applied force and the bending displacement at fracture were measured and depicted. The maximal applied force allows an estimation of the implants' strength, whereas the ductility of the pins is shown by the different bending displacement values at fracture. As this was a not-standardized bending test, the results could only be compared among themselves.

μ-Computed tomography

To estimate the modification of the implants' cross sections, the samples were analysed using X-ray tomography (μCT80, Comp. Scanco Medical, Zurich, Switzerland). After fixing the bone-implant composite with foam cubes in a plastic tube, the sample was scanned with 10 μm resolution, amperage of 145 μA and voltage of 55 kV. Integration time was 498 ms.

The resulting tomograms served for the creation of 3D geometrical bodies. Using the software IPL (image processing language, Comp. Scanco Medical), these bodies were filled with "globes" which were adapted to the bodies' cross sections. The change in cross-sectional diameter was visualized by miscoloured depiction.

Scanning electron microscopy

SEM allowed an examination of the implants' surface with regard to the surface rearrangement, the adsorption of tissue and the changes in the composition of the material. The latter was determined by using EDX. SEM and EDX examinations were carried out at LEO1455VP (Comp. LEO, XY) before and after the treatment with hydrofluoric acid. The chamber vacuum was 1.04×10^{-5} with a voltage of 20 kV and a jet stream of 30 μA. The applied detector was the Rutherford Back-Scattered Detector. The degradation of the pins was evaluated with a 30-fold magnification. Following this, the surface was scanned with a magnification of 100–1000-fold magnification to describe changes. Interesting changes and residues were analysed by EDX to determine their element composition. For the EDX analysis, a death time of 40–60% and an operating distance of approx. 15 mm were applied. Each EDX measurement lasted a minimum of 75 lifeseconds which equates to 3 min. The following elements were included: magnesium, calcium, phosphorus, carbon, oxygen, sodium, potassium, chloride, titanium and the alloy-specific elements aluminium, yttrium and the rare earth metals lanthanum, cerium and neodymium.

To evaluate the degradation layer, cross sections which were produced for metallographic investigations were likewise analysed by EDX. Since the embedding mass partly infiltrated the degradation layer, the element composition of the embedding mass was determined as well. The evaluation software was EDAX Genesis (Comp. AMETEK, Germany).

Metallography

The metallographic micrographs in the initial state of the implants as well as after 3 and 6 months implantation period served for characterization of the material and its micro-structural changes. Therefore, the organic layer was left on the surface. The implants were embedded in epoxy resin and afterwards grinded to a surface roughness of 1 μm and polished. To depict the precipitations, 2% nitric acid was applied. Following their evaluation, a second grinding process and etching was added to visualize grain boundaries. This etching was carried out using a solution of 7 g nitroxanthic acid and 9 mL acetic acid.

All pictures were taken with the reflected light microscope Axioplan 2 (Comp. Zeiss, Germany).

Experimental results

Clinically, all implant materials were very well tolerated. The animals showed neither signs of pain nor lameness.

Radiographical examination could not reveal any gas generation within the muscle tissue or under the skin during the whole implantation period.

Determination of volume

All implants showed a decrease in volume during the implantation period (Fig. 1). The mean initial volume was similar for all magnesium alloys (MgCa0.8 0.125 ± 0.005 cm^3; LAE442 0.125 ± 0.005 cm^3; WE43 0.127 ± 0.006 cm^3).

All in all, MgCa0.8 implants showed the highest loss in volume. Although the mean value after 3 months (0.112 ± 0.002 cm^3) was slightly higher than that of LAE442 pins, the residual mean volume reached only 0.078 ± 0.004 cm^3 after 6 months and was therewith the lowest of the three alloys. LAE442 implants showed the strongest loss in volume during the first 3 months. The mean value decreased for 15% to 0.106 ± 0.01 cm^3. After 6 months implantation duration, the mean implant volume was 0.097 ± 0.003 cm^3. Hence, after the longer implantation period LAE442 implants showed the least loss in volume of all investigated alloys. The moderate loss in volume of WE43 (0.116 ± 0.005 cm^3) within the first 3 months resembled the MgCa0.8 implants. However, after 6 months, the decrease proceeded strongly. Consequently, the values (0.082 ± 0.01 cm^3) were lower than for LAE442 implants.

Three-point bending test

All three alloys showed significant differences regarding their mechanical strength (Fig. 2). In the initial state, MgCa0.8 implants had the least strength of all (178.76 ± 25.15 N). After 3 months implantation period, a distinct decrease to 115.42 ± 9.66 N could be seen, which further proceeded obviously after 6 months (52.90 ± 5.96 N). LAE442 implants beard the highest load of all materials in their initial state (255.67 ± 5.69 N). They also showed a

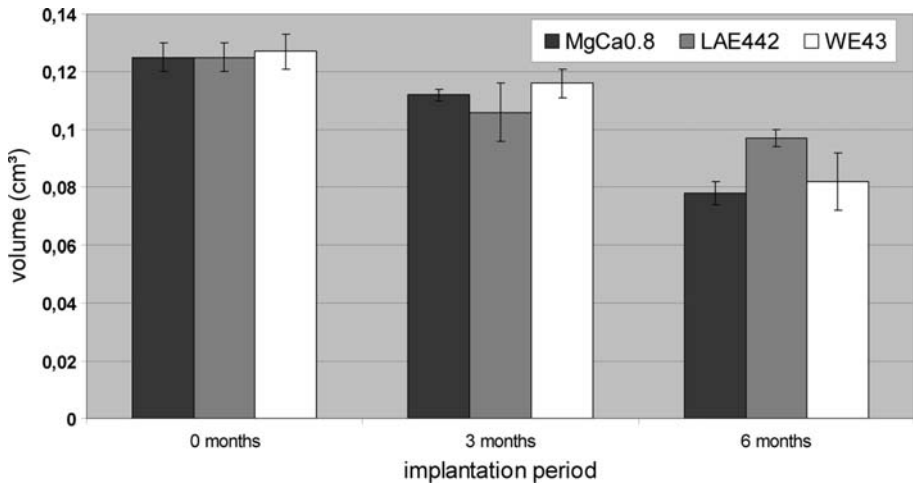

Fig. 1 Volume determination of the three magnesium alloys MgCa0.8, LAE442 and WE43 in their initial state and after 3 and 6 months implantation duration

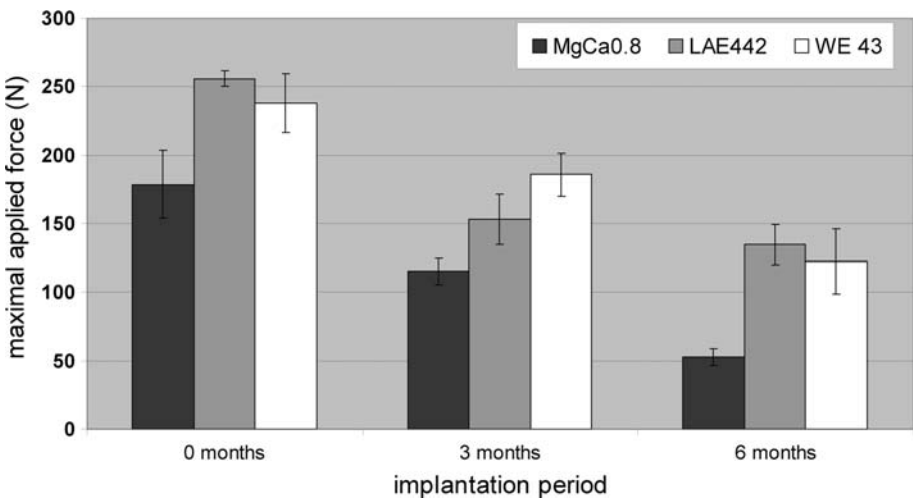

Fig. 2 Maximal applied force of the magnesium alloys MgCa0.8, LAE442 and WE43 at their initial state and after 3 and 6 months implantation duration

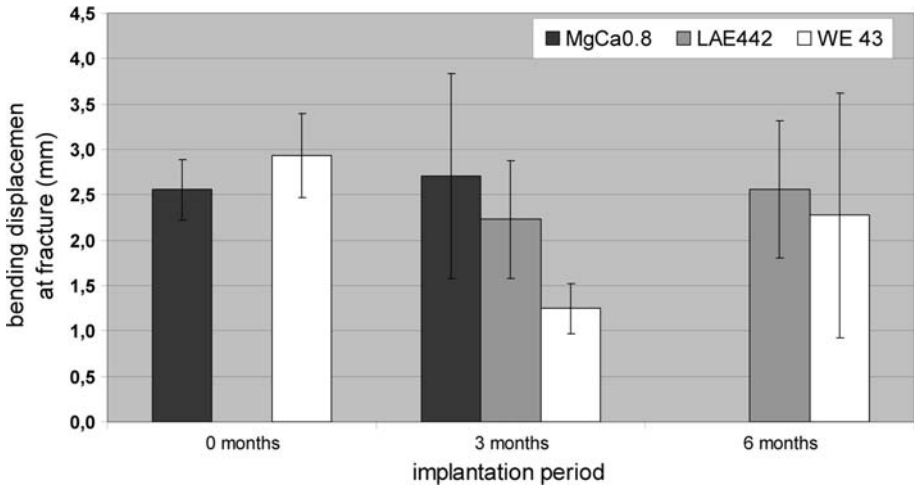

Fig. 3 Bending displacement at fracture of the magnesium alloys MgCa0.8, LAE442 and WE43 in their initial state and after 3 and 6 months implantation duration

decrease in strength during both implantation periods. After 3 months, the loss in strength was 40% to 153.21 ± 18.45 N, and therewith relatively high, whereas after 6 months, the further decrease was much slower with 7% to 134.68 ± 14.68 N. The initial strength values of WE43 (238.05 ± 21.68 N) implants were higher than MgCa0.8 pins but lower than LAE442 implants. They showed the least decrease in strength after 3 months (185.59 ± 15.64 N). After 6 months, the loss in strength proceeded relatively constantly. They reached values of 122.23 ± 23.65 N.

The results were inhomogeneous regarding the bending displacement at fracture to evaluate the implants' ductility (Fig. 3). In their initial state, MgCa0.8 reached the fracture criterion at a bending displacement of 2.56 ± 0.33 mm. After 3 months, the bending displacement at fracture elongated slightly to 2.7 ± 1.13 mm. None of the MgCa0.8 implants reached the fracture criterion after 6 months. The force decreased slowly and constantly until it reached a loss in force of 10% and the test was terminated. The bending displacement at that point was lower than 5 mm. Consequently, the graphical depiction is lacking since no value was given for the bending displacement at fracture. All initial LAE442 implants reached a bending displacement of 5 mm without a decrease in the maximal applied force. Hence, they did not fulfil the fracture criterion when the test was terminated and no graphical depiction was made. After 3 months implantation duration, the fracture occurred at a bending displacement of 2.23 ± 0.65 mm. After 6 months, the bending displacement elongated marginally to 2.56 ± 0.75 mm. WE43 fulfilled the fracture criterion in their initial state as well as after 3 and 6 months implantation period. In their initial state, the bending displacement at fracture was 2.93 ± 0.46 mm and therefore higher than in MgCa0.8. After 3 months, the bending displacement decreased obviously to 1.25 ± 0.28 mm. A distinct increase in bending displacement could be seen after 6 months implantation duration (2.27 ± 1.35 mm).

X-ray tomography

Due to the degradation of the material, a decrease in the cross-sectional dimension generally occurred for all materials as implantation time increased (Fig. 4). The cross-sectional dimension of MgCa0.8 already varied after 3 months. These variations significantly increased after a period of 6-month implantation. The occurring strong pitting corrosion led to distinct differences in the cross-sectional diameter. LAE442 only showed slight changes in their cross-sectional diameter after 3 months. After 6 months, they showed an advanced decrease in diameter, but the changes over the length of the implant were less serious than in MgCa0.8 implants. Furthermore, no pitting corrosion could be found. After 3 months, WE43 implants showed a similar degradation as LAE442 implants. In contrast, several parts of the implant developed pitting corrosion as MgCa0.8 pins (Fig. 5). After 6 months implantation period, they showed an obvious reduced

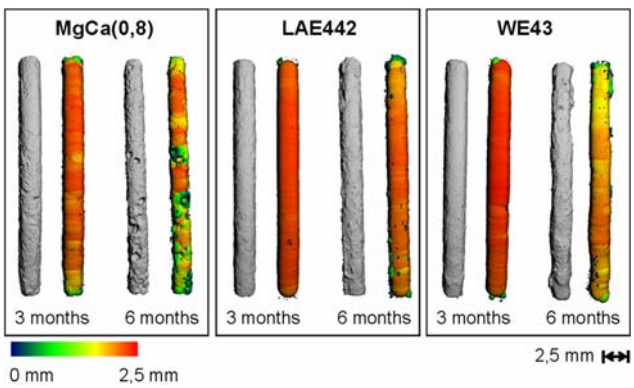

Fig. 4 μ-Computed tomography miscoloured illustrations of the magnesium alloys MgCa0.8, LAE442 and WE 43 after 3 and 6 months implantation duration. The cross-sectional diameter is depicted in different colours according to its value (software IPL, ScancoMedical)

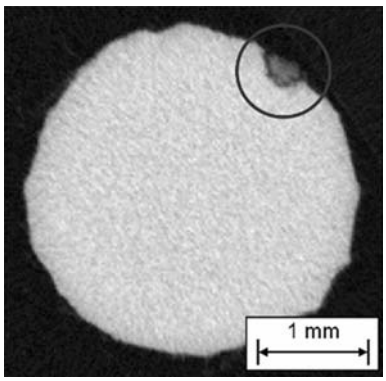

Fig. 5 μ-Computed tomography cross section of a WE43 implant after 3 months implantation period. At the upper image part, the typical pitting corrosion could be seen (*circle*)

cross-sectional diameter, which was very inhomogeneous over the implants' length.

Scanning electron microscopy and energy dispersive X-ray analyses

Before treating the pins with hydrofluoric acid, the surface of the implants contained residues of tissue and corrosion products.

For MgCa0.8 pins, a trabecular structure covered parts of the surface, both after 3 and 6 months. The structure consisted of magnesium, phosphorus and calcium in equals parts. After 3 months, LAE442 implants showed hemispherical-shaped prominences (Φ approx. 200 µm). Furthermore, fan-shaped, needle-like structures were visible. EDX analysis revealed that these structures consisted of magnesium, phosphorus and calcium in equal parts, according to the MgCa0.8 implants. The surface of WE43 pins showed none of these structures. Only organic material could be found. It was recognizable that the underlying implant surface started to peel off clod-likely. After 6 months, the peeling was more pronounced.

After the treatment with hydrofluoric acid, the surface morphology of the implants could be examined directly. Due to degradation, different surface morphologies appeared for the three materials. The surface of MgCa0.8 is characterized by pitting corrosion which was more distinct after 6 months. The surface of LAE442 had a lamellar structure. WE43 showed soil-like ablations on the surface. In LAE442 and WE42, ligaments appeared as well. They were of different dimensions and randomly distributed over the surface. Under higher magnification, all three magnesium alloys showed puniest porosities on the surface after 6 months implantation period.

A qualitative analysis of the degradation layer (Fig. 6) was carried out using EDX analysis of the cross sections (Table 1).

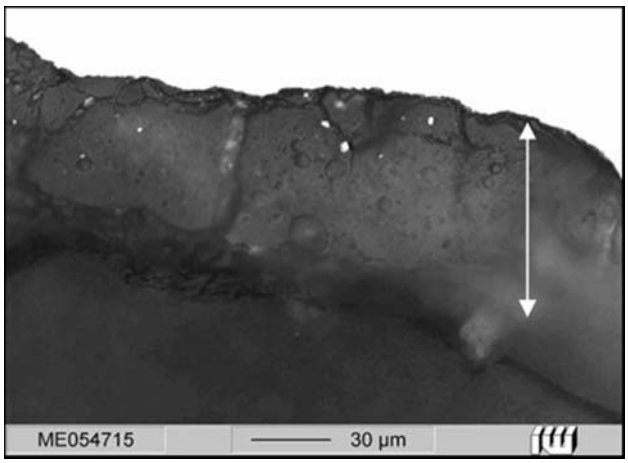

Fig. 6 Part of a metallographic cross section of the degradation layer of a LAE442 implant. The *white spots* are precipitations of rare earth metals

Table 1 Results of the EDX-analysis of the degradation layer of MgCa0.8, LAE442 and WE43 implants after 3 and 6 months implantation duration

Element	wt% 3 Months			wt% 6 Months		
	MgCa0.8	LAE 442	WE 43	MgCa0.8	LAE 442	WE 43
Magnesium	25.98	22.01	23.83	18.11	18.28	20.53
Phosphorus	3.22	3.27	0.78	2.15	2.79	0.3
Calcium	6.34	2.01	2.9	3.8	3.02	2.66
Yttrium	n.m.	n.m.	4.96	n.m.	n.m.	3.28
Rare earths	n.m.	1.71	n.m.	n.m.	2.71	n.m.
Neodymium	n.m.	n.m.	n.m.	n.m.	n.m.	1.93
Aluminium	n.m.	2.91	n.m.	0.15	3.42	0.2
Silicon	1.72	1.74	1.85	0.09	0.2	0.38
Carbon	36.07	41.38	36.2	54.52	41.99	54.03
Oxygen	26.69	24.96	27.06	20.02	26.75	15.84
Chloride	6.34	n.m.	n.m.	0.41	0.26	0.31
Potassium	n.m.	n.m.	n.m.	0.47	0.27	0.44
Sodium	n.m.	n.m.	0.11	0.29	0.08	0.12

n.m. not measured

The analysis of the embedding material showed mainly carbon and oxygen. Furthermore, magnesium and chloride could be detected in small amounts. Hence, chloride, oxygen and carbon could not be included into the evaluation of the degradation layer. It is likely that magnesium was distributed on the surface during the preparation (grinding, burnishing) of the samples and therefore could be also detected in the embedding material.

The evaluation of aluminium and silicon had to be done carefully, too, as these elements were included in the grinding medium and in the abrasive.

Irrespective of the material, the layer primarily consisted of magnesium, calcium, phosphorus and organic fractions. As

expected, MgCa0.8 implants showed significantly higher amounts of calcium than both other alloys after 3 months implantation period. After 6 months, this difference had disappeared. Aluminium could not be found in the layer of MgCa0.8 and WE43 implants after 3 months implantation duration. In contrast, LAE442 implants showed a distinct amount of aluminium after 3 months. After 6 months implantation period, aluminium amounts were higher for all alloys and still significantly richer in content in LAE442 pins. An obvious difference could also be found regarding the content of chloride. After 3 months, distinct amounts appeared in the degradation layer of MgCa0.8 implants. None of the other alloys showed chloride amounts after this implantation period. After 6 months, all implants showed similar contents of chloride in the degradation layer. Another general difference in the composition of the layer was detected for the elements sodium and potassium. Both only existed after an implantation period of 6 months irrespective of the alloy. Traces of potassium were detectable after 3 months only for WE43.

Metallography

Micrographs of the implants before and after the two implantation periods were used to determine any changes in microstructure. As expected, the composition of the material did not change in the surface zone. The distribution of precipitation in the samples was only visible as etching was applied. MgCa0.8 implants showed longish precipitations spread out over the whole material. After 3 months, the rare earths containing alloys LAE442 and WE43 revealed production derived, longitudinally elongated precipitations of rare earth metals. Cross-directional, these precipitations appeared to be punctiform, light spots.

Through resin embedding and preparation of cross-sectional polishes, the degradation layer could be demonstrated and evaluated. The evaluation revealed an increase in layer thickness with increasing implantation period for all investigated materials.

The etching with nitroxanthic and acetic acid did not reveal any favoured degradation at the grain boundaries.

Discussion

The aim of this study was to examine whether previously tested magnesium alloys have the required mechanical and degradation properties for the use as degradable bone implant material. For this purpose, a determination of volume, three-point bending tests, μ-computed tomography, SEM examinations including EDX analysis and metallographic examinations were carried out.

The determination of volume showed that the degradation progress of MgCa0.8 implants is advantageous. Within the first 3 months, the pins degraded slowly. The following 3 months, the degradation rate accelerated so that the decrease in volume reached 40% after 6 months. LAE442 implants degraded slower than both other alloys. Apparently, the degradation rate decreased with increasing implantation duration. WE43 showed a similar behaviour as MgCa0.8 implants but the values varied highly after 6 months. Xu et al. [23] also reported on results regarding the loss in volume of magnesium-based implants. They examined magnesium–manganese–zinc–alloy implants which were inserted into the femora of rats. After 18 weeks implantation duration, the pins degraded nearly 50%. Also Li et al. [24] could show that MgCa1.0 implants hold only one-third of their initial weight after an implantation period of 3 months. An initially slow degradation rate followed by acceleration after an appropriate time would be advantageous. Hence, subsequent studies will focus on the further degradation progress of LAE442 implants during longer implantation periods. Stagnation of degradation would be undesirable. Therefore, in a further study corresponding LAE442 pins will be implanted in the same manner for a longer time (9 and 12 months) and examined under the same conditions to see how the degradation proceeds further and if the pins are finally resorbed. Linearity of the further degradation progress would be preferable.

The three-point bending tests revealed that all alloys showed different results regarding their strength and ductility. The mechanical properties altered depending on the degradation period. Comparable investigations are lacking in the accessible literature. The MgCa-system had the least strength in its initial state as well as after 3 and 6 months of implantation duration. However, the ductility of the implant remained to a large extend. LAE442 showed good mechanical properties all in all. The implants had the highest strength and the best ductility in their initial state. The ductility decreased with increasing implantation duration. However, after 6 months, the bending displacement at fracture corresponded to that of MgCa0.8 samples. In the context of osteosynthesis of weight-bearing bones, a higher mechanical strength is advantageous to a constant ductility as the implants primary have to stabilize the bone fragments. WE43 did not show a constant decline in strength depending on the implantation period. The results varied attributable to surface effects and cross-sectional inhomogeneities. Due to local pitting corrosion after 3 months, the implants' cross section was weakened. The brittle fracture behaviour of WE43 implants could also be caused by an increased liability of cracking. After an implantation period of 6 months, some WE43 samples showed a ductile material behaviour again. The elongation at fracture was even better than at the initial state. Although the surface was fissured no massive pitting corrosion could be found any more. The displacement at fracture might rise

due to the reduced implant diameter. Thus, equal applied forces led to a higher bending.

μ-Computed tomography examinations revealed strong, cross-sectional inhomogeneities depending on the alloy and the implantation period. Pitting corrosion could mainly be found in most slices of the MgCa0.8 implants. LAE442 pins degraded homogeneously at the boundaries of the implants. The cross-sectional diameter did not change obviously. WE442 implants had similar degradation behaviour as LAE442, but some areas of the pins showed intense pitting corrosion as in MgCa0.8. Reports on μ-computed tomography examinations for evaluation of the degradation behaviour of osteosynthetic implants are scarce. von der Höh et al. [25] rated the degradation progress and shape by μ-computed tomography. Thus, they were able to show that rougher MgCa implants degrade faster than smooth implants. Also Witte et al. [26] evaluated the degradation progress of magnesium-based implants by synchrotron μ-computed tomography. They showed that the corrosion rate (CR) could be described by the reduction of volume (ΔV) divided by the multiplied implantation period (t) and implant cross section (A) ($CR = \Delta V/t^*A$). Both studies showed in a different way that μ-computed tomography is a reasonable technique to evaluate the degradation behaviour. This study also succeeded in appraising the different kinds of degradation of magnesium alloy implants. Especially, the cross sections give information about the degradation progress and type. Thus, unfavourable pitting corrosion could be found in MgCa0.8 and some of the WE43 implants.

The SEM-analyses revealed that the implants developed different surface morphologies. As in the μ-computed tomography, pitting could be found on the surfaces of MgCa0.8 implants represented by the holey and irregularly removed surface. Due to the fact that besides metallography, pitting corrosion could also be found in other examination methods (e.g. μ-computed tomography), the theory of etching as cause of pitting corrosion could be abandoned. Song and Atrens [27] described pitting corrosion as typical for the corrosion of magnesium. Witte et al. [28] reported on pitting corrosion of LAE442 implants. Pitting corrosion was not found for LAE pins in this study. Currently, no reasons for the line-like surface structure of LAE442 implants and the circular structure of WE43 pins are known. After 6 months of implantation, little porosities covered the whole surface of all investigated implants. A possible reason might be that trabecular bone infiltrated the implants there. Some authors reported on the osteoinductive tendency of magnesium alloys [29, 30]. Examinations on magnesium-based cylinders with different surface properties could show that depending on the implants' surface a close bone-to-implant contact could be seen after both 3 and 6 months implantation period in the medial femoral condylus of rabbits [31]. Therefore, an infiltration of the implant with trabecular bone might be possible.

Also EDX analysis close to implants and their periphery [23, 28, 32] is an adequate and often used technique and enables an evaluation of a potential osteoinductive effect [28]. In this study, the degradation layer mainly consisted of the elements phosphorus, calcium and magnesium. Phosphorus and calcium are fundamental components of the bone. Also Witte et al. [28] reported on an amorphous calcium phosphate layer on in vivo degraded magnesium implants. Due to the existence of Ca and P in the degradation layer in this study, it can be assumed that osteogenesis or a pre-stage of osteogenesis is initiated. Subsequent investigations over a longer implantation period have to verify this assumption. After an implantation time of 6 months, sodium and potassium could also be found in the layer. Both elements are involved in metabolism processes. An explanation might be that lower metabolism processes had taken place after 3 months so that K and Na could only be detected after 6 months implantation period.

The metallographic investigations of the pins revealed the formation of a degradation layer for all magnesium alloy implants after both implantation periods. This is in accordance with several studies concerning the degradation of magnesium [23, 24, 33, 34]. In this study, the layer's thickness (100–250 µm) is dependent on the material and the implantation time. Etching for evaluating grain boundaries did not give any hints whether corrosion is stronger at these interfaces. For rare earth-containing alloys, the precipitations of the metal substrate were integrated into the degradation layer. This indicates that the organism was hardly able to degrade or metabolize the rare earth components within 6 months. In contrast, Witte et al. [28] found that the rare earth metals neodymium and cerium were distributed homogeneously within in vivo degraded magnesium implants. No rare earths could be detected within the bone tissue. They concluded logically that the rare earth metals were dissolved and did not accumulate in the bone. So far, this apparent contradiction could not be explained. One possible reason might be found in the different production processes, resulting in different geometries of the implants. Different production processes such as cold working or heat treatment influence the properties of metals. This could result in different grain sizes, boundaries or precipitations which on their part could lead to a different degradation behaviour. As no results on metallurgical examinations including grain size or boundaries are known for the implants used by Witte et al., the production processes could only be a hypothesis for the different amounts of rare earth elements within the degradation layer. Further investigation thereon will have to be done.

Conclusion

MgCa0.8 shows an insufficient initial strength and a fast degradation. Although its ductility is constant and the degradation products can be regarded as harmless as they are natural components of the organism, its use as degradable osteosynthesis material for weight-bearing bones seems to be limited.

LAE442 degraded slowly and its initial strength seems to be sufficient for an application in weight-bearing bones. The rare earth elements, which are apparently hard to resorb, might have previously unknown effects. Further investigations on the release of these degradation products and their biocompatibility are necessary.

The mechanical properties and the degradation behaviour of WE43 implants are unpredictable and therefore, it is ineligible for the use as implant material.

Besides further examinations on rare earth-containing alloys, magnesium-based alloy systems with lithium, aluminium and calcium should be investigated.

Acknowledgement This study is part of the collaborative research centre (SFB599, Medical University of Hannover, University of Veterinary Medicine Hannover and University of Hannover), which is sponsored by the German Research Foundation (DFG).

References

1. Hofmann GO (1995) Arch Orthop Trauma Surg 114:123
2. Meyer-Lindenberg A, Pruss M, Fehr M, Brunnberg L (1996) Prakt Tierarzt 77:987
3. Rehm KE, Helling HJ, Gatzka C (1997) Orthopade 26:489
4. Moses PA, Lewis DD, Lanz OI, Stubbs WP, Cross AR, Smith KR (2002) Aust Vet J 80:336
5. Syrcle JA, Cook JL (2004) Vet Comp Orthop Traumatol 17:121
6. Long M, Rack HJ (1998) Biomaterials 19:1621
7. Disegi JA, Eschbach L (2000) Injury 31(Suppl 4):2
8. Wintermantel E, Ha S (1998) Biokompatible Werkstoffe und Bauweisen. Springer, Berlin
9. Raiha JE (1992) Clin Mater 10:35
10. Kannan MB, Raman RK (2008) Biomaterials 29:2306
11. Aluminium-Zentrale Düsseldorf (2000) Magnesiumtaschenbuch. Aluminium, Düsseldorf
12. Wolff J (1892) Das Gesetz der Transformation der Knochen. Hirschwald, Berlin
13. Turner CH (1992) J Biomech 25:1
14. Tsubota K, Suzuki Y, Yamada T, Hojo M, Makinouchi A, Adachi T (2009) J Biomech 42(8):1088
15. Verbrugge J (1934) La Press Med 23:460
16. Switzer E (2005) Resorbierbares metallisches Osteosynthesematerial. Dissertation, Stiftung Tierärztliche Hochschule, Hannover
17. Krause A, Hackenbroich C, von der Höh N, Wagner S, Bormann D, Hassel T, Windhagen H, Meyer-Lindenberg A (2005) Biomaterialien 6:190
18. Witte F, Michael B, Klement M, Goede F, Wirth CJ, Windhagen H (2005) In: Transactions of the 51st Annual Meeting of the Orthopaedic Research Society, Washington, DC. http://www.ors.org/web/Transactions.asp; No. 0989
19. Sha M, Guo Z, Fu J, Li J, Yuan CF, Shi F, Li SJ (2009) Acta Orthop 80:135
20. Uctasli MB, Arisu HD, Lasilla LV, Valittu PK (2008) Eur J Dent 2:263
21. Meyer-Lindenberg A, Krause A, Krause C, Bormann D, Windhagen H (2007) Biomaterialien 8:180
22. Lass J (2005) Untersuchungen zur Entwicklung einer magnesiumgerechten Strangpresstechnologie. Books on demand, Norderstedt
23. Xu L, Yu G, Zhang E, Pan F, Yang K (2007) J Biomed Mater Res A 83:703
24. Li Z, Gu X, Lou S, Zheng Y (2008) Biomaterials 29:1329
25. von der Höh N, Krause A, Hackenbroich C, Bormann D, Lucas A, Meyer-Lindenberg A (2006) Dtsch Tierarztl Wochenschr 113:439
26. Witte F, Fischer J, Nellesen J, Crostack HA, Kaese V, Pisch A, Beckmann F, Windhagen H (2006) Biomaterials 27:1013
27. Song G, Atrens A (1999) Adv Eng Mater 1:11
28. Witte F, Kaese V, Haferkamp H, Switzer E, Meyer-Lindenberg A, Wirth CJ, Windhagen H (2005) Biomaterials 26:3557
29. Revell P, Damien E, Zhang X, Evans P, Howlett C (2004) Key Eng Mater 254–256:447
30. Song G, Atrens A (2003) Adv Eng Mater 5:837
31. von der Höh N, Bormann D, Lucas A, Denkena B, Hackenbroich C, Meyer-Lindenberg A (2009) Adv Eng Mater 11:B47
32. Acarturk O, Lehmicke M, Aberman H, Toms D, Hollinger JO, Fulmer M (2007) J Biomed Mater Res B Appl Biomater. doi: 10.1002/jbm.b.30987
33. Pardo A, Merino MC, Coy AE, Arrabal R, Viejo F, Matykina E (2008) Corros Sci 50:823
34. Rettig R, Virtanen S (2008) J Biomed Mater Res A 85:167